

Chapter 4

Isotope Labeling Methods for Relaxation Measurements

Patrik Lundström, Alexandra Ahlner, and Annica Theresia Blissing

Abstract Nuclear magnetic spin relaxation has emerged as a powerful technique for probing molecular dynamics. Not only is it possible to use it for determination of time constant(s) for molecular reorientation but it can also be used to characterize internal motions on time scales from picoseconds to seconds. Traditionally, uniformly ^{15}N labeled samples have been used for these experiments but it is clear that this limits the applications. For instance, sensitivity for large systems is dramatically increased if dynamics is probed at methyl groups and structural characterization of low-populated states requires measurements on $^{13}\text{C}\alpha$, $^{13}\text{C}\beta$ or ^{13}CO or $^1\text{H}\alpha$. Unfortunately, homonuclear scalar couplings may lead to artifacts in the latter types of experiments and selective isotopic labeling schemes that only label the desired position are necessary. Both selective and uniform labeling schemes for measurements of relaxation rates for a large number of positions in proteins are discussed in this chapter.

4.1 Introduction

Nuclear magnetic resonance (NMR) spin relaxation is a powerful tool for identifying and quantifying molecular dynamics on multiple time scales. For instance, measurements of the longitudinal (R_1) and transverse (R_2) auto-relaxation rates and the heteronuclear nuclear Overhauser enhancement (NOE) allows determination of the rotational diffusion tensor as well as characterization of the time scale and magnitude of bond vector motions through model-free analysis [1–3]. Slower motions on the μs -ms time-scale, often corresponding to larger structural rearrangements important for processes like protein folding, enzymatic catalysis and ligand binding can also be studied using Carr-Purcell-Meiboom-Gill (CPMG) [4, 5] and $R_{1\rho}$ [6, 7] relaxation dispersion. In these experiments the excess contribution to transverse relaxation is modeled in terms of exchange rates and chemical shift differences between exchanging states. In principle, all NMR active nuclei can be used as probes in relaxation experiments although some are more useful than others for reasons of simplicity, sensitivity and ease of interpretation. For instance, if the exchange contribution to transverse relaxation is quantified it is beneficial if this contribution is large compared to other contributions, which in practice excludes quadrupolar

P. Lundström (✉) • A. Ahlner • A.T. Blissing
Division of Molecular Biotechnology, Department of Physics,
Chemistry and Biology, Linköping University, SE-58183 Linköping, Sweden
e-mail: patlu@ifm.liu.se

nuclei. On the other hand, for quadrupolar nuclei other relaxation mechanisms than the quadrupolar coupling can be disregarded, which simplifies the analysis.

In practice, all relaxation experiments involving proteins and other biomolecules require isotopic labeling. The most commonly used isotopic labeling schemes are uniform labeling with ^{15}N and/or ^{13}C . For reasons that are explained below, these methods are useful for the measurement of relaxation rates for certain positions in proteins while they fail for others. Different selective labeling techniques that can be used in these cases, advantages and disadvantages with these will also be discussed.

To be useful, a labeling scheme should optimally meet as many as possible of several, sometimes conflicting, criteria. For example, all desired sites should be labeled with high yield, sites that would interfere with experiments should not be labeled, the labeling protocol should be simple to implement, protein yields should be high, the isotopically labeled precursors should be cheap and as few different samples as possible should be required. The possibility to use certain samples for several different experiments should be exploited and the use of simple strategies such as uniformly ^{15}N , $^{13}\text{C}/^{15}\text{N}$ or $^{13}\text{C}/^{15}\text{N}/\text{H}$ labeled samples for certain relaxation experiments should not be overlooked.

4.2 Spin Relaxation and Chemical Exchange

4.2.1 Spin Relaxation

Relaxation is due to the stochastic modulation of spin couplings resulting from molecular motion. The quadrupolar coupling usually dominates relaxation for spins $I > 1/2$ while for spins $I = 1/2$ the most important relaxation mechanisms are due to dipole-dipole coupling and the chemical shift anisotropy. Relaxation can be described at different levels of rigor from the phenomenological description by the Bloch equations [8] to a fully quantum-mechanical treatment [9]. It turns out that a semi-classical approach, in which the spins are treated quantum-mechanically and the lattice is treated classically leads to correct answers for most relevant cases [10]. Application of this theory shows that relaxation for coupled spins is described by a set of coupled differential equations where cross-correlation and cross-relaxation lead to interconversion of operators and multi-exponential decays whereas absence of such mechanisms lead to mono-exponential decays. All relaxation rate constants are given by the coupling strength multiplied with a weighted sum of spectral densities. These are usually modeled according to the model-free formalism that takes global tumbling as well as internal motions on two time-scales faster than the global tumbling into account [1–3]. In the case of isotropic diffusion, the expression for the spectral density is then given by

$$J(\omega) = \frac{2}{5} \left[\frac{S^2 \tau_c}{1 + (\omega \tau_c)^2} + \frac{(1 - S_f^2) \tau_f'}{1 + (\omega \tau_f')^2} + \frac{(S_f^2 - S^2) \tau_s'}{1 + (\omega \tau_s')^2} \right] \quad (4.1)$$

where $S^2 = S_f^2 S_s^2$; S_f^2 and S_s^2 are the generalized order parameters for fast and slow internal motions, respectively; $\tau_f' = \tau_f \tau_c / (\tau_f + \tau_c)$; $\tau_s' = \tau_s \tau_c / (\tau_s + \tau_c)$; τ_f and τ_s are the correlation times for the fast and slow internal motions respectively and τ_c is the correlation time for molecular tumbling.

The most common relaxation parameters measured to model protein dynamics are the longitudinal (R_1) and transverse (R_2) auto-relaxation rates and the heteronuclear NOE [11] that are given by Eqs. 4.2, 4.3, 4.4, and 4.5.

$$R_1 = \frac{d^2}{4} [3J(\omega_I) + 6J(\omega_I + \omega_S) + J(\omega_I - \omega_S)] + c^2 J(\omega_I) \quad (4.2)$$

$$R_2 = \frac{d^2}{8} [4J(0) + 3J(\omega_I) + 6J(\omega_S) + 6J(\omega_I + \omega_S) + J(\omega_I - \omega_S)] + \frac{c^2}{6} [4J(0) + 3J(\omega_I)] \quad (4.3)$$

$$\sigma_{IS} = \frac{d^2}{4} [6J(\omega_I + \omega_S) - J(\omega_I - \omega_S)] \quad (4.4)$$

$$NOE = 1 + \frac{\sigma_{IS}}{R_1} \cdot \frac{\gamma_S}{\gamma_I} \quad (4.5)$$

where $d = \mu_0 \hbar \gamma_I \gamma_S \langle r_{IS} \rangle^{-3} / 4\pi$; $c = \gamma_I B_0 \Delta\sigma / \sqrt{3}$; μ_0 is the permeability of vacuum; \hbar is the reduced Planck constant; γ_I and γ_S are the magnetogyric ratios; r_{IS} is the internuclear distance; B_0 is the static magnetic field strength and $\Delta\sigma$ is the anisotropy of the (axially symmetric) chemical shift tensor.

For spins $I=1/2$ the auto-relaxation rates depend on dipolar and chemical shift anisotropy. It can be shown that if there are no cross-correlations between these mechanisms, the decay of transverse magnetization is mono-exponential as desired. However, for longitudinal magnetization the dipolar interaction with another spin will lead to cross-relaxation. Similarly, the NOE will not be quantitated accurately if the spin belongs to a dipolar coupled network. Cross-correlations between dipole-dipole and chemical shift anisotropy mechanisms or different dipole-dipole mechanisms also lead to multi-exponential decays that prevent the extraction of accurate parameters. These problems can however be corrected by inverting the dipolar field of the coupled nucleus by 180° pulses at appropriate time-points during the relaxation delay. For backbone ^{15}N positions this is an easy task and dedicated pulse sequences that lead to minimal errors have been described [11, 12]. The reason why this is feasible is because relaxation in this case is totally dominated by the interaction with the attached proton and the ^{15}N chemical shift anisotropy. Importantly, the ^{15}N spin is isolated from other ^{15}N spins in the sense that such dipolar and scalar couplings are vanishingly small. For the other two common spin $I=1/2$ nuclei in proteins, ^{13}C and ^1H , the situation is less favorable and the naive approach of using uniformly labeled samples for these experiments often fails. For measurements of transverse relaxation rates an additional concern is the homonuclear scalar coupling.

4.2.2 Chemical Exchange

Chemical exchange is the result of a stochastic modulation of the chemical shift on a time scale that is slower than the correlation time for molecular tumbling. This modulation may indeed be due to chemical reactions as the name suggests but more commonly it results from conformational exchange that for proteins include processes like folding, ligand binding and enzymatic catalysis [13–15]. Chemical exchange manifests as an excess contribution to transverse relaxation and thus line broadening and is classified as slow, intermediate or fast depending on the size of the exchange rate constant in relation to the difference in resonance frequencies between exchanging states. The maximal information that can be extracted from measurements of exchange broadening is the populations of all exchanging states as well as exchange rate constants and (the magnitude of) the difference in resonance frequencies between exchanging states as shown in Eq. 4.6. If chemical exchange is fast on the chemical shift time-scale, the exchange contribution to transverse relaxation, R_{ex} , for exchange between sites A and B is

$$R_{ex} = \frac{p_A p_B \Delta\omega_{AB}^2}{k_{ex}} \quad (4.6)$$

where P_A and P_B are the populations of the exchanging states, $\Delta\omega_{AB}$ is the difference in resonance frequencies for states A and B and $k_{ex} = k_{AB} + k_{BA}$ is the exchange rate constant. For slow exchange, R_{ex} for states A and B equals k_{AB} and k_{BA} , respectively, whereas a considerably more complicated equation governs intermediate exchange.

Chemical exchange on the intermediate to fast time-scale is measured by Carr-Purcell-Meiboom-Gill (CPMG) [16, 17] or $R_{1\rho}$ [18, 19] relaxation dispersion experiments where the effective transverse relaxation rate $R_{2,eff}$ is a function of the effective field of either a CPMG pulse train or the amplitude and offset of the spinlock field. The obtained dispersion profiles are fitted to the Bloch-McConnell equations [20], either numerically or to expressions that cover special cases [21, 22]. To characterize slow exchange, ZZ-exchange experiments are commonly employed [23]. These experiments only report on the exchange rate between exchanging states but all chemical shifts are, of course, readily obtained from the peak positions in the spectra.

As for measurements of fast dynamics, most studies hitherto have focused on using ^{15}N as a probe for millisecond dynamics. However, since excited state chemical shifts can be extracted from the experiments and the chemical shifts can be used as restraints in structure calculations [24–26] it is highly desirable to measure relaxation dispersions also for other nuclei to characterize protein excited states structurally. Another reason for measurements on different nuclei is to increase the confidence in the extracted parameters when fitting the data to more complex models like three-site exchange [27].

In CPMG experiments, scalar coupling evolution may result in artifacts for at least two reasons. First, the relaxation rates of in-phase and anti-phase operators may be very different, especially if the coupled nucleus is a proton. If care is not taken, the magnetization will spend different amounts of time in-phase and anti-phase, even during a constant time delay, depending on the number of refocusing pulses that are applied and the effective relaxation rate is thus not only modulated by chemical exchange. Relaxation compensation elements that explicitly average in-phase and anti-phase relaxation rates for all choices of the number of CPMG pulses [4] or continuous wave decoupling of the coupled nucleus to keep the magnetization in-phase [5] minimize artifacts when these techniques can be applied. Both these methods are however hard to apply if the coupled nuclei are of the same species. A second problem in the homonuclear case is that the scalar coupling evolves differently in the slow and fast pulsing limits since the spins get increasingly more strongly coupled as the pulsing rate increases. In $R_{1\rho}$ experiments Hartmann-Hahn transfer for certain choices of offset and amplitude of the effective field present a similar problem. The reason for the widespread use of backbone ^{15}N as a probe for molecular dynamics largely is that one does not need to be concerned with such problems.

Another way to eliminate problems associated with homonuclear scalar couplings is to let the coupled nuclei evolve as multiple-quantum operators during the relaxation delay since this renders the scalar coupling between the nuclei inactive. Multiple-quantum relaxation rates typically report on cross-correlated couplings. These may be cross-correlations between two different dipole-dipole interactions, two chemical shift anisotropy interactions or one dipole-dipole and one chemical shift anisotropy interaction. Multiple-quantum relaxation rates thus report on the angle between the principal frames of the two couplings and can be used to obtain information on dihedral angles in proteins [28, 29]. In the case of fast exchange, the excess contribution to the difference between double-quantum and zero-quantum contributions, $\Delta R_{MQ,ex}$, is given by

$$\Delta R_{MQ,ex} = \frac{4P_A P_B \Delta\omega_I \Delta\omega_S}{k_{ex}} \quad (4.7)$$

where P_A and P_B are the populations for states A and B and $\Delta\omega_I$ and $\Delta\omega_S$ are the associated differences in resonance frequencies for spins I and S [30]. It is noteworthy that $\Delta R_{MQ,ex}$ is four times as sensitive to chemical exchange as R_{ex} (single-quantum) if $\Delta\omega_I$ and $\Delta\omega_S$ are of similar magnitude.

An interesting feature of cross-correlated chemical exchange is that $\Delta R_{MQ,ex}$ reports on the relative signs of $\Delta\omega_I$ and $\Delta\omega_S$.

To measure the above mentioned parameters using NMR spectroscopy, the protein sample requires isotopic labeling. Some experiments require very precise positioning of labels, which will be reviewed later on. First, we turn to the metabolic pathways responsible for amino acid synthesis in *E. coli* to shine light on how these pathways can be utilized for labeling purposes.

4.3 Biosynthesis of Amino Acids

Since proteins used for NMR are samples almost exclusively produced by over expression in *E. coli*, the focus will be on over expression in this organism. Cell-free synthesis will be discussed briefly at the end of this chapter. To appreciate how different labels are incorporated into specific positions in proteins we must study how amino acids are synthesized. The main references for this section are the textbooks in biochemistry by Voet and Voet [31] and in bacterial metabolism by Gottschalk [32].

Working backwards from the amino acids, the last step of biosynthesis is typically transamination of the corresponding α -ketoacid where the amide group is derived from Gln or Glu and the α -proton from solvent. Specifically this means that the isotopic composition at H α will be identical to the solvent composition, ignoring kinetic isotope effects. Nitrogen is usually supplied to the growth medium in the form of NH_4Cl so that enrichment with ^{15}N is achieved by using $^{15}\text{NH}_4\text{Cl}$ as the nitrogen source.

The precursors for the α -ketoacids of all amino acids are surprisingly few. Working from the more complex ones to the more simple ones we have phosphoenolpyruvate and erythrose-4-phosphate (Phe, Trp, Tyr), ribose-5-phosphate (His, Trp), α -ketoglutarate (Arg, Gln, Glu, Pro), oxaloacetate (Asp, Asn, Lys, Met, Thr), pyruvate (Ala, Leu, Lys) and 3-phosphoglutarate (Gly, Ser, Cys). If we want to know from which molecules most positions in amino acid residues are derived it suffices to know the biosynthesis of these compounds. It turns out that 3-phosphoglutarate, phosphoenolpyruvate and pyruvate are intermediates in glycolysis, oxaloacetate is produced either from carboxylation of phosphoenolpyruvate or from the tricarboxylic acid (TCA) cycle. The precursor α -ketoglutarate is exclusively produced in the TCA cycle. Positions 4 and 5 of this molecule are derived from acetyl-S-CoA while positions 1–3 are derived from positions 4–2 of oxaloacetate (note the descending order in the latter case). The precursors for the aromatic side-chains are intermediates of the pentose phosphate pathway.

The three metabolic pathways will be reviewed briefly and are presented in Figs. 4.1, 4.2, and 4.3. To illustrate the concepts of selective labeling and scrambling, the carbon atom initially at position 2 of glucose is highlighted in red.

4.3.1 Glycolysis

Glycolysis starts with the conversion of glucose to 1,3-bisphosphofruuctose through two intermediates. This molecule is subsequently cleaved into dihydroxyacetonephosphate and glyceraldehydephosphate. While dihydroxyacetonephosphate is a dead end in the biosynthesis of amino acids, this molecule is readily interconverted into glyceraldehydephosphate when this pool is depleted. Glyceraldehydephosphate is oxidized into pyruvate through a number of intermediates two of which are 3-phosphoglutarate and phosphoenolpyruvate. The carbons at positions 1–3 of these molecules, which are identical to positions 1–3 or 6–4 (note the descending order in the latter case) of glucose, correspond to CO, C α and C β , respectively, for the amino acids derived from glycolytic intermediates.

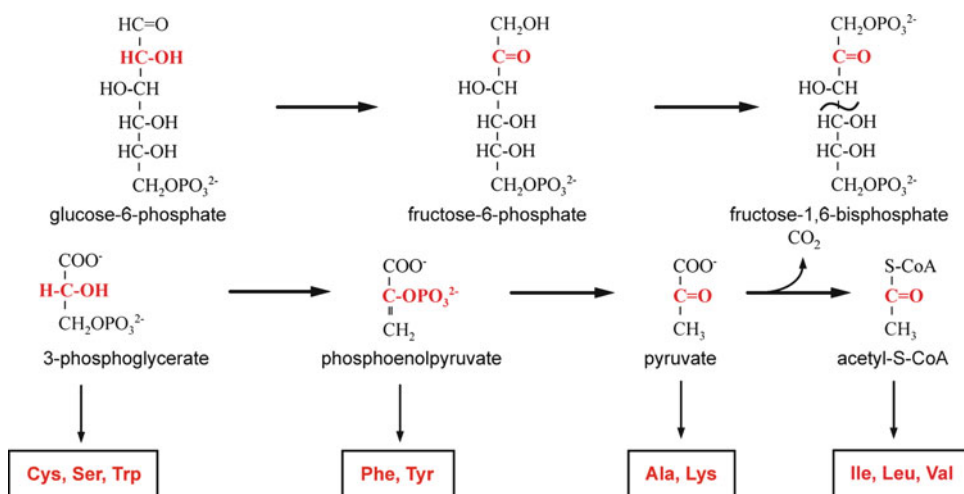


Fig. 4.1 Glycolysis. Carbon atoms originally at position 2 of glucose are highlighted in red. Steps that are of little relevance to the text are not shown. Amino acids derived from various intermediates are indicated

4.3.2 The TCA Cycle

The starting point for the TCA cycle (Fig. 4.2) is oxaloacetate that may be the product from the previous pass of the cycle or synthesized by carboxylation of pyruvate or phosphoenolpyruvate. The labeling might thus be different depending on the relative fluxes of these pathways and will also depend on the isotopic composition of bicarbonate in the solvent. Oxaloacetate is fused to acetyl to yield citrate which isomerizes and is subsequently decarboxylated at position 1 of oxaloacetate, to yield α -ketoglutarate, the precursor of Glu, Gln, Arg and Pro. α -ketoglutarate is decarboxylated, so that the position corresponding to position 4 of oxaloacetate leaves, to yield succinate. Through three intermediates succinate in turn is converted back to oxaloacetate. It is noteworthy that while succinate is symmetric in the sense that positions 1 and 4 as well as positions 2 and 3 are equivalent, oxaloacetate is not. This adds more complexity to the labeling patterns of amino acids.

4.3.3 The Pentose Phosphate Pathway

The pentose phosphate pathway serves multiple purposes, including being a source of reducing power (NADPH) and to provide the cell with building blocks for nucleotides and aromatic amino acids. As is seen in Fig. 4.3, it comprises multiple steps and except for the oxidative steps all are readily reversible. How the pentose phosphate pathway is run is thus dependent on the requirements of the cell. For instance, if NADPH is needed the pentose phosphate pathway is run forward as indicated in the figure whereas if building blocks are needed it may be run in reverse by the use of fructose-6-phosphate and glyceraldehyde-3-phosphate as substrates. The resulting labeling patterns for applicable amino acids thus depend on the relative balance of these modes.

The oxidative branch of the pentose phosphate pathway involves decarboxylation of position 1 from 6-phosphogluconate to yield ribulose-5-phosphate that is readily isomerized to ribose-5-phosphate and xylulose-5-phosphate. In the non-oxidative branch, these pentoses combine to form first seduheptalose-7-phosphate and glyceraldehyde-3-phosphate and then erythrose-4-phosphate and fructose-6-phosphate. Erythrose-4-phosphate is used in the biosynthesis of the amino acids Phe, Trp and Tyr but it can also combine with xylulose-5-phosphate to give fructose-6-phosphate and glyceraldehyde-3-phosphate.

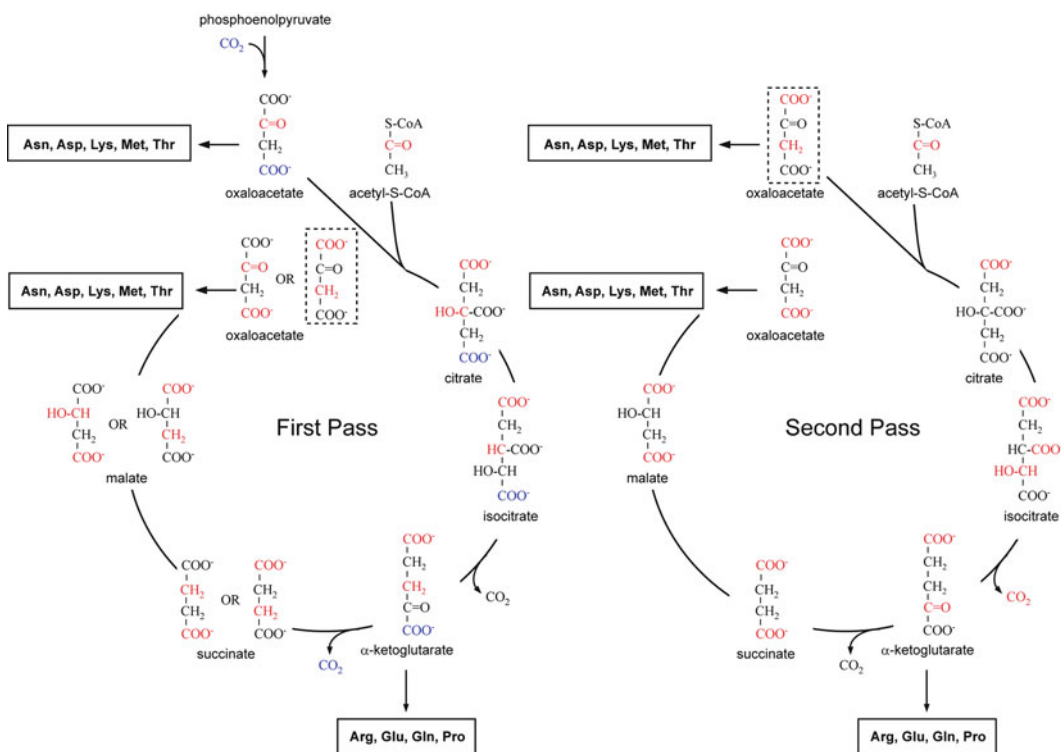


Fig. 4.2 The TCA cycle. Two passes are shown and the amino acids derived from the intermediates oxaloacetate and α -ketoglutarate are indicated. Some steps of little relevance to this text have been omitted. Carbon atoms originally at position 2 of glucose are highlighted in red and the carbon atom originating from carbon dioxide is shown in blue. Residues that are derived from the intermediates oxaloacetate and α -ketoglutarate are indicated. It is noteworthy that C α for the residues derived from oxaloacetate and C β for the residues derived from α -ketoglutarate are isotopically enriched in the first pass of the cycle whereas C α for the α -ketoglutarate group of residues is enriched in the second pass

4.3.4 Scrambling

Scrambling of label may result from additional pathways than those considered but also from the complexity of the considered pathways themselves. For example, in the TCA cycle oxaloacetate can be produced by carboxylation of phosphoenolpyruvate but also as the last step in the cycle. By simply following the fate of various carbon atoms in the two cases it is clear that the labeling pattern may be different (Fig. 4.2). Furthermore, the oxaloacetate product in one pass of the cycle can be used as substrate in the next pass, yielding yet another labeling pattern. The isotopomer composition of the amino acids derived from oxaloacetate may thus be extremely complex. The same considerations hold for the amino acids derived from α -ketoglutarate.

The pentose phosphate pathway is even more prone to scrambling since several of the reactions are rapid and readily reversible. This applies to the isomerization of the pentoses and also by the transaldolase and transketolase reactions. Hence, the pathway can, and is, run in different modes depending on the cellular demands. The isotopomer compositions of amino acids made from building blocks of the pentose phosphate pathway are thus notoriously hard to predict. It should also be noted that the products of the pentose phosphate pathway, fructose-6-phosphate and glyceraldehyde-3-phosphate, are glycolytic intermediates that might be labeled differently than if produced in glycolysis, as illustrated in Figs. 4.1 and 4.3.

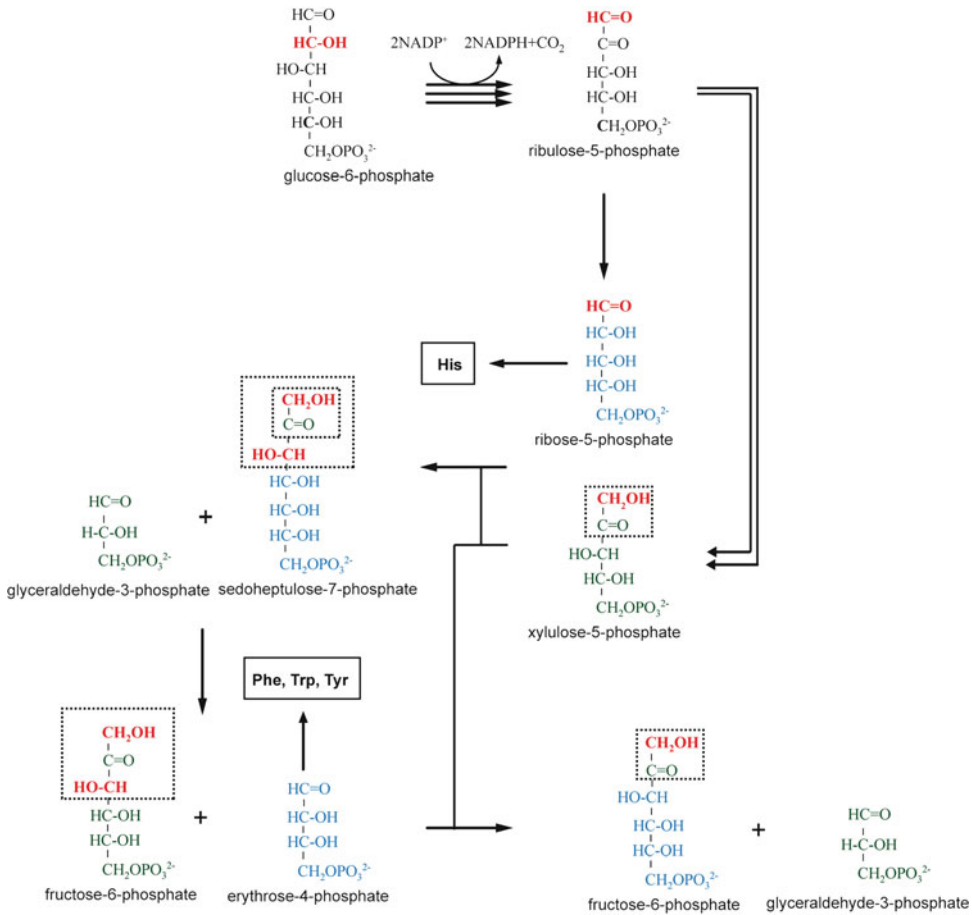


Fig. 4.3 The pentose phosphate pathway. Carbon atoms originally at position 2 of glucose are highlighted in red. Other color coding and boxes are used to keep track of which fragments that are used for the different positions of the various compounds. Amino acids that are derived from pentose phosphate pathway intermediates are indicated

4.4 Protein Expression and Purification

Isotopically enriched proteins are usually expressed in M9 minimal medium [33], referred to as M9 medium in the following. M9 medium is primarily composed of 6 g/L Na₂HPO₄, 3 g/L KH₂PO₄ and 0.5 g/L NaCl. These salts are dissolved in H₂O or D₂O or a mixture of the two depending on labeling scheme. This medium is supplemented with 1 mM MgSO₄, 0.1 mM CaCl₂, 10 mg/L biotin, 10 mg/L thiamine and antibiotics. Depending on labeling scheme, stock solutions for these components should be dissolved in H₂O or D₂O. A carbon source, most commonly 2–3 g/L glucose, and a nitrogen source, almost always 0.5–1 g/L NH₄Cl are also added to the medium. An expression protocol that has frequently been used to produce uniformly and selectively labeled samples is as follows [34]:

1. Transfer one or more freshly transformed *E. coli* colonies of BL21(DE3) strain to 30 mL LB (in H₂O) supplemented with the appropriate antibiotic(s) and grow cells at 37°C in a shaking incubator until OD₆₀₀ = 1.0 is reached.
2. Spin down the cells at 1,200 × g, 15 min. at room temperature (25°C).

3. Resuspend a fraction of the cells in 10% of the isotopically labeled M9 medium to achieve OD_{600} of 0.1–0.2. Grow the cells at 37°C until $OD_{600} = 1.0$. Pour the starter culture directly into the remaining 90% of the isotopically enriched M9 medium.
4. Grow the cells at 37°C until $OD_{600} = 0.6–1.0$.
5. Induce over expression with 0.5–1 mM IPTG. Perform over expression either at 37°C for 2–5 h or at room temperature or 16°C overnight. The final OD_{600} will depend on the growth medium and on the duration of over expression. This step should be modified if selectively labeled precursors or amino acids are used. In this case these compounds are added to the growth medium 1 h before over expression is induced.

Purification is usually performed by lysing the cells and subjecting the lysate to different methods of chromatography. These include affinity chromatography, ion-exchange chromatography and size-exclusion chromatography. A particular concern is when the protein has to be purified from inclusion bodies. In this case the inclusion bodies must be solubilized in 6 M GdnCl or 8 M urea after lysis. After a preliminary purification step, the protein is refolded and purification is then continued. Refolding is done by exchange to a buffer that favors the folded state and can be performed by several different methods including dialysis, on column or by rapid dilution [35]. The refolding protocol typically has to be optimized differently for each protein. Denaturation and refolding is also usually necessary if complete exchange of protons to deuterons, or vice versa, at amide positions is required.

4.5 Labeling at Specific Positions in Proteins

4.5.1 Backbone and Side-Chain Nitrogen Positions

For completeness the discussion will start by ^{15}N since it is the most common probe for molecular dynamics for a number of reasons. For HSQC-type experiments involving ^{15}N relaxation it suffices to produce a uniformly ^{15}N labeled sample by expression in M9 medium where 0.5–1 g/L $^{15}\text{NH}_4\text{Cl}$ is the sole nitrogen source using the protocol outlined above. Experiments measuring ^{15}N R_1 , R_2 and the $[^1\text{H}]-^{15}\text{N}$ NOE [11, 12] and interpreted according to the model-free formalism [1–3] have been the standard method for estimating the diffusion tensor and the backbone flexibility of proteins since the early 1990s. Backbone ^{15}N positions have also been used extensively to study microsecond to millisecond dynamics in proteins. Relaxation compensated CPMG pulse sequences that average relaxation of in-phase and anti-phase operators equally regardless of the repetition rate of the refocusing pulses [4] during a constant time relaxation delay [36] means that artifact-free ^{15}N CPMG dispersions can be recorded. For exchange rates in excess of a few thousand per second, rotating-frame dispersion experiments are better suited [6]. The experiments can be designed to measure $R_{1\rho}$ - R_1 as suggested originally or the pure $R_{1\rho}$ rate [37].

Since nitrogen also is present in some side-chains these positions can also be studied and they can be used to probe formation and disruption of salt-bridges (Arg, Lys) and to monitor protonation/deprotonation (His).

Although not required, the experiments for quantifying dynamics on all time-scales work equally well for samples that are also labeled with ^{13}C . This is useful since this means that the $^{13}\text{C}/^{15}\text{N}$ labeled sample usually used for resonance assignments and NOESY experiments can be used to measure relaxation at ^{15}N sites. As will be described below, such samples can also be used to probe dynamics at carbonyl and certain other positions. Furthermore, perdeuteration, achieved by using deuterated glucose as the carbon source and 100% D_2O for protein expression, dramatically enhances sensitivity for large proteins. A very versatile sample is thus a uniformly $^{13}\text{C}/^{15}\text{N}/^2\text{H}$ labeled sample with deuterium at amide positions back exchanged to protons.

Table 4.1 Chemical shift ranges and scalar coupling constant for selected ^{13}C positions in proteins

Position	Chemical shift range (ppm)	Homomuclear one-bond couplings
^{13}CO	170–180	$J_{\text{COA}} = 55$ Hz
$^{13}\text{C}\alpha$	40–70	$J_{\text{CAO}} = 55$ Hz, $J_{\text{CAB}} = 35$ Hz
$^{13}\text{C}\beta$	15–75	$J_{\text{BCA}} = 35$ Hz, $J_{\text{BCG}} = 35$ Hz
$^{13}\text{C}^{\text{methyl}}$	5–30	$J_{\text{CC}} = 35$ Hz
$^{13}\text{C}^{\text{aromatic}}$	120–150	$J_{\text{CC}} = 60$ Hz

4.5.2 Carbon Positions

For the other important heteronucleus, ^{13}C , the situation is more complicated. All uniformly ^{13}C -labeled amino acid residues except Gly comprise spin systems of at least three, $\text{C}\alpha$, $\text{C}\beta$ and CO , scalar coupled ^{13}C nuclei. The chemical shift range and important scalar couplings for different positions are given in Table 4.1. The one bond scalar coupling constant between $^{13}\text{C}\alpha$ and ^{13}CO is 55 Hz, between aliphatic ^{13}C positions it is 35 Hz and between aromatic ^{13}C positions it is around 60 Hz. In addition there may be significant three-bond couplings, notably between $^{13}\text{C}^{\text{methyl}}$ and $^{13}\text{C}\alpha$ for Leu residues and between $^{13}\text{CO}^{\text{backbone}}$ and $^{13}\text{CO}^{\text{side-chain}}$. Different strategies need to be employed depending on which nucleus that is probed and this section will be a survey of different labeling schemes and tricks in pulse sequences needed to probe dynamics of many of these positions in relaxation experiments. Although simultaneous labeling by ^{15}N is not necessary except for in experiments where magnetization is transferred through this nucleus it is useful to routinely include it in any labeling scheme since it facilitates a convenient ^{15}N -HSQC check of sample integrity.

4.5.2.1 ^{13}CO at Backbone and Side-Chains Positions

The backbone ^{13}CO chemical shift is sensitive to the backbone dihedral angles and can be used as a probe for secondary structure whereas the side-chain ^{13}CO chemical shift reports on electrostatic interactions. In addition, the relaxation properties of this nucleus are quite favorable compared to other ^{13}C positions in protonated samples. Another simplifying feature compared to other ^{13}C positions is that for $^{13}\text{CO}^{\text{backbone}}$ the only covalently bound carbon is $\text{C}\alpha$. From Table 4.1 it follows that they resonate approximately 15 kHz apart already at a static magnetic field of 11.7 T. It is thus feasible to manipulate ^{13}CO and $^{13}\text{C}\alpha$ separately using band-selective RF-pulses. This was utilized by Ishima et al. who designed a HNC0-type CPMG experiment for the measurement of ^{13}CO relaxation dispersions in a uniformly $^{13}\text{C}/^{15}\text{N}$ labeled sample and found good correlation between extracted rate constants from ^{13}CO and ^{15}N CPMG experiments [38]. One scalar coupling that was not refocused in the pulse sequence was the three bond coupling between backbone ^{13}CO and side-chain ^{13}CO in Asx residues. This manifested as artifacts for residues of these types since the coupling evolves differently in the slow and fast pulsing limits. This issue was addressed in a later communication describing a similar CPMG experiment for backbone ^{13}CO sites in proteins [39]. By including a refocusing element (termed J-refocusing element) in the middle of the CPMG period it was possible to selectively invert the side-chain but not backbone ^{13}CO so that the coupling was refocused by the end of the CPMG period. This effectively removed the problem with artifacts resulting from these couplings. Another method of measuring ^{13}CO dispersions on uniformly labeled samples was reported by Mulder and Akke who developed a rotating-frame relaxation experiment and measured R_2 rates for the proteins calbindin $\text{D}_{9\text{k}}$ and the E140Q mutant of the C-terminal domain of calmodulin [40].

If desired, selective labeling of CO backbone positions in proteins can be achieved by using 3 g/L $[3\text{-}^{13}\text{C}]$ -pyruvate and 3 mM $\text{NaH}^{13}\text{CO}_3$ as the carbon sources in the growth medium [41]. The use of

labeled bicarbonate increases the fractional incorporation of label for residue types derived from α -ketoglutarate (Fig. 4.2). This strategy leads to a fractional incorporation of label of 70–90% for residues derived from glycolytic intermediates and about 25% for residues derived from TCA cycle intermediates. The only residue type that is not significantly labeled is Leu. It has however been shown that the pairwise root-mean-square-deviation of extracted excited state chemical shifts from measurements on selectively and uniformly labeled samples is essentially zero [39]. Because of this there are few reasons to use the selective labeling strategy since a uniformly labeled sample provides superior sensitivity, is more versatile and that the complication due to $^{13}\text{CO}_{\text{backbone}}\text{-}^{13}\text{CO}_{\text{side-chain}}$ scalar couplings can be circumvented by including the J-refocusing element. The presence of the three bond $^{13}\text{CO}_{\text{backbone}}\text{-}^{13}\text{CO}_{\text{backbone}}$ coupling for adjacent residues is a concern for both labeling strategies although it is scaled down, especially for some pairs of residue types, using the selective labeling.

Uniform or partial deuteration of aliphatic and aromatic positions is not required for these experiments but is still useful since the sensitivity increases somewhat for small proteins and more dramatically so for larger ones, especially if the strategy is combined with TROSY type experiments. A $^{15}\text{N}/^{13}\text{C}/^2\text{H}$ labeled sample can additionally be used for measurements of amide proton relaxation rates (described below). One sample can thus be used to probe dynamics for three different nuclei for all amino acids except Pro (or residues preceding Pro in the case of ^{13}CO).

Uniformly ^{13}C labeled samples can also be used to measure millisecond dynamics at ^{13}CO side-chain positions in proteins. In a recent application Hansen and Kay measured CPMG dispersions for ^{13}CO side-chains in uniformly labeled proteins [42]. Similar concerns as for backbone positions apply and the J-refocusing element described above was included to refocus couplings to backbone ^{13}CO .

4.5.2.2 $^{13}\text{C}\alpha$ Positions

For $^{13}\text{C}\alpha$, the situation is significantly more complicated. In addition to the coupling to ^{13}CO , which can be refocused, one must consider the coupling to $^{13}\text{C}\beta$, which in general cannot. This necessitates the development of selective labeling schemes that label $^{13}\text{C}\alpha$ but not $^{13}\text{C}\beta$. This can be done in different ways. Perhaps the simplest approach is to use randomly ^{13}C labeled glucose as the carbon source. This will result in some isolated $^{13}\text{C}\alpha$ positions (or as $^{13}\text{C}\alpha\text{-}^{13}\text{CO}$ spin-pairs which can be handled using band-selective pulse) and some problematic $^{13}\text{C}\alpha\text{-}^{13}\text{C}\beta$ spin pairs. A related method based on using a mixture of differently labeled acetate molecules has also been described by Wand et al. who used 15% $[2\text{-}^{13}\text{C}]\text{-acetate}$, 15% $[2\text{-}^{13}\text{C}]\text{-acetate}$ and 70% unlabeled acetate and measured relaxation rates at various carbon positions in ubiquitin [43]. The main drawback of these methods is that the pulse sequence must contain an element that edits out $^{13}\text{C}\text{-}^{13}\text{C}$ spin pairs. This introduces a fixed delay in the pulse sequences, leading to reduced sensitivity. Furthermore, the approach is not effective in yielding a large fraction of isolated $^{13}\text{C}\alpha$ moieties.

A significantly better approach was proposed by LeMaster and Kushlan [44]. They used a bacterial strain deficient in the enzymes *sdh-1* and *mdh-1* as to disrupt the TCA cycle to reduce scrambling and used $[2\text{-}^{13}\text{C}]\text{-glycerol}$ as the carbon source for expression. They reported high levels of isotopic enrichment at $\text{C}\alpha$ without simultaneous enrichment at $\text{C}\beta$ for 13 residue types. Ile and Val were highly enriched at $\text{C}\alpha$ but unfortunately also at $\text{C}\beta$. The only residues that were not enriched were Arg, Gln, Glu, Leu and Pro using this strategy. However, also these can get highly enriched at $\text{C}\alpha$ if a second sample is prepared by expression in the same strain with $[1,3\text{-}^{13}\text{C}_2]\text{-glycerol}$ as the carbon source. Thus, if two different samples are produced, $^{13}\text{C}\alpha$ relaxation rates can be measured for all residue types except Ile and Val. This labeling scheme has since been the major method for obtaining samples with alternate $^{13}\text{C}\text{-}^{12}\text{C}$ labeling for solid state NMR applications [45]. It has not yet been established whether the method can be used for recording artifact-free $^{13}\text{C}\alpha$ CPMG dispersions. That has however been established using a similar strategy based on 3 g/L $[2\text{-}^{13}\text{C}]\text{-glucose}$ as the carbon source and ordinary BL21(DE3) cells [41, 46]. Using this labeling scheme and a pulse sequence optimized for

$^{13}\text{C}\alpha$ dispersions, accurate excited state chemical shifts could be extracted for an SH3 domain from Abp1p. Also, clean mono-exponential decays were observed in R_1 and $R_{1\rho}$ experiments for ubiquitin showing that cross-correlation and cross-relaxation artifacts are absent. The obvious drawback with this method compared to the one of LeMaster and Kushlan is that incorporation of label is only half as effective. There are however a few things that speak in its favor. The first is that one sample suffices for relaxation measurements involving 17 residue types. Additionally, faster growth rates and higher protein yields are expected using glucose as the carbon source in cells with an intact TCA cycle.

In $R_{1\rho}$ experiments the weak form of the homonuclear scalar coupling is inactive and by clever positioning of the RF-carrier, magnetization transfer due to the strong scalar coupling can be scaled down sufficiently to not constitute a problem even for uniformly ^{13}C labeled samples. Yamazaki et al. showed that accurate measurements of $R_{1\rho}$ could indeed be obtained at $^{13}\text{C}\alpha$ positions for all amino acid residues except Ser and Thr on uniformly ^{13}C labeled samples whereas measurements of R_1 and the heteronuclear $[^1\text{H}\alpha]$ - ^{13}C NOE were more troublesome because of cross-correlation and cross-relaxation effects [47]. The $R_{1\rho}$ measurements involving uniformly ^{13}C labeled samples have subsequently been extended to probe microsecond-millisecond dynamics for $^{13}\text{C}\alpha$ positions in proteins [48].

4.5.2.3 $^{13}\text{C}\beta$ Positions

For $\text{C}\beta$ an analysis of glycolysis and the TCA cycle shows that the inverse of the schemes for labeling $\text{C}\alpha$ should be effective at obtaining high level enrichment for many residue types. Thus using $[1,3\text{-}^{13}\text{C}_2]$ -glycerol or $[1\text{-}^{13}\text{C}]$ -glucose as the carbon source should be workable strategies. In the case of relaxation experiments involving $\text{C}\beta$ it is in general not sufficient that $\text{C}\alpha$ positions stay unlabeled but the same must also apply for $\text{C}\gamma$. It turns out that even when only considering the TCA cycle it is not feasible to get isolated $^{13}\text{C}\beta$ moieties for certain residue types as shown in Fig. 4.4.

LeMaster and Kushlan used the cell-line described above with two lesions in the TCA cycle to prevent scrambling and measured $^{13}\text{C}\beta$ relaxation rates for a sample of thioredoxin produced by over expression with $[1,3\text{-}^{13}\text{C}_2]$ -glycerol as the carbon source [44]. Kay and co-workers implemented a similar strategy with 3 g/L $[1\text{-}^{13}\text{C}]$ -glucose as the main carbon source in a cell-line in which *sdh-1* was knocked out [49]. To reduce the extent of carboxylation of phosphoenolpyruvate with labeled carbon dioxide, $^{12}\text{CO}_2$ was added to the medium in the form of 20 mM natural abundance sodium bicarbonate. Figure 4.4 shows there will be no $^{13}\text{C}\beta$ - $^{13}\text{C}\alpha$ or $^{13}\text{C}\beta$ - $^{13}\text{C}\gamma$ spin-pairs as a result of scrambling in the TCA cycle if it is disrupted this way. Unfortunately only 11 residue types will be labeled to more than 30% using this strategy. However, four additional residue types are available if an additional sample using 3 g/L $[2\text{-}^{13}\text{C}]$ -glucose as the carbon source is produced (Fig. 4.2). In this case there is no need for using bacterial strains with lesions in the TCA cycle although the use of such strains leads to increased fractional incorporation of label, perhaps at the expense of slower growth rates and overall lower protein yields.

The current methodology for specific labeling at $\text{C}\beta$ positions is far from optimal which is evident from the limited number of $^{13}\text{C}\beta$ relaxation experiments that have been reported. A further complicating issue with this position is that there are one, two or three attached protons depending on residue type, necessitating three different versions of pulse sequences for the relaxation experiments in order to probe all residue types [49].

4.5.2.4 Methyl Side-Chains

Methyl side-chains are attractive probes for molecular dynamics since they provide high sensitivity and are ubiquitous in well-folded proteins. In many relaxation experiments it is necessary that covalently linked carbon positions are not isotopically labeled and several methods for achieving this have

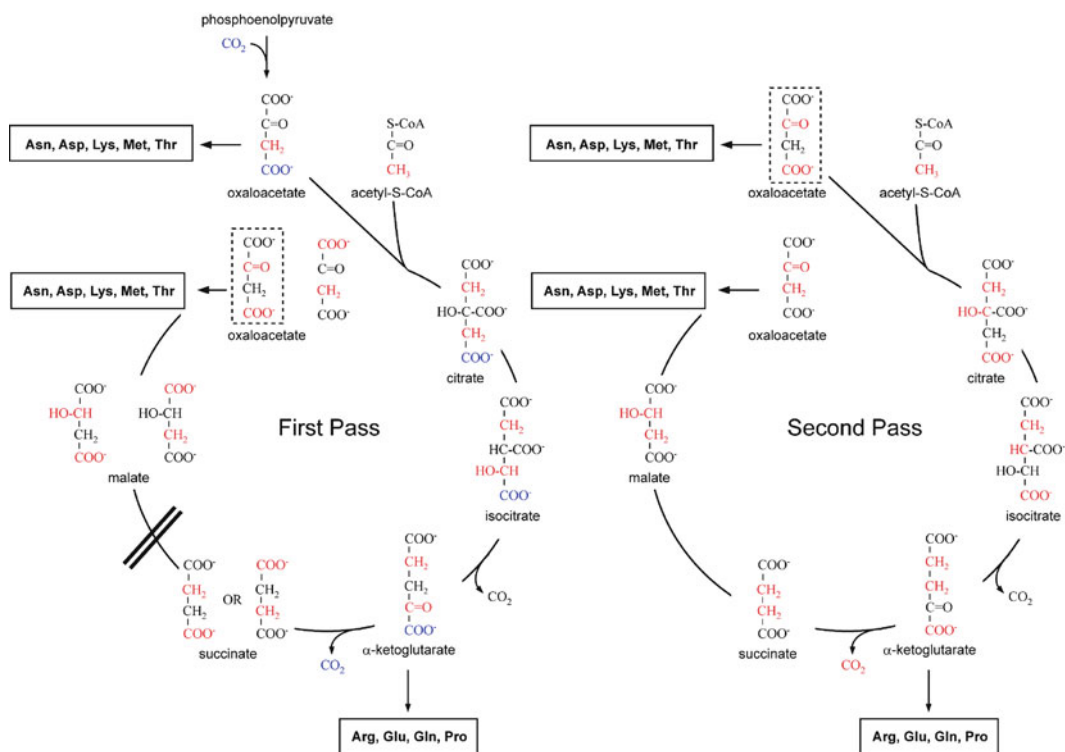


Fig. 4.4 Illustration of scrambling of label in the TCA cycle if [1- ^{13}C]-glucose is used as the carbon source. Carbon positions originally at position 1 of glucose are highlighted in red and carbon dioxide that is used to phosphorylate phosphoenolpyruvate is colored blue. The double slash indicates the end point of the pathway if the enzyme succinate dehydrogenase is knocked out

been proposed. Because the methyl group of Met is isolated from other carbon nuclei, selective ^{13}C labeling at the methyl groups is not necessary and uniformly ^{13}C labeled samples can be used for relaxation experiments [50]. A simple and cheap strategy to obtain isolated ^{13}C methyl groups for most other cases is to use 3 g/L [1- ^{13}C]-glucose as the carbon source. A straightforward analysis of the biosynthetic pathways shows that this leads to enrichments of almost 50% at the methyl side-chains of Ala, Leu, Val, and Ile γ 2 without enrichment at neighboring carbon nuclei [46]. This strategy has been used to record methyl CPMG dispersions for proteins of different sizes such as the FF domain from human FBP11, 71 residues, 8.6 kDa, and a complex between *E. coli* NAD(P)H:FRE, 232 residues, 27 kDa and FAD [51, 52].

The same methyl side-chains can also be labeled using other strategies. Mulder et al. used [3- ^{13}C]-pyruvate as carbon source which results in close to 100% incorporation of label at the above mentioned methyl side-chains [53]. The degree of incorporation of label is thus doubled compared to if [1- ^{13}C]-glucose is used. However, it should be noted that [3- ^{13}C]-pyruvate is significantly more expensive and that bacterial growth is slow using this carbon source, perhaps with reduced protein yields as a result. Contrary to when [1- ^{13}C]-glucose was used the authors noted scrambling for Ala residues resulting in a mixture of $^{12}\text{C}\alpha$ - $^{13}\text{C}\beta$ and $^{13}\text{C}\alpha$ - $^{13}\text{C}\beta$ spin-pairs. Contributions to the NMR signal from the latter can however be removed by incorporation of an editing element into the pulse sequence, causing decreased sensitivity [53]. The scheme suggested by LeMaster and Kushlan, using [1,3- $^{13}\text{C}_2$]-glycerol as the carbon source [44] should produce similar results.

A cleaner way of selectively labeling certain methyl side-chains is to add the commercially available compounds α -ketobutyrate (precursor of Ile) and/or α -ketoisovalerate (precursor of Leu, Val) that are

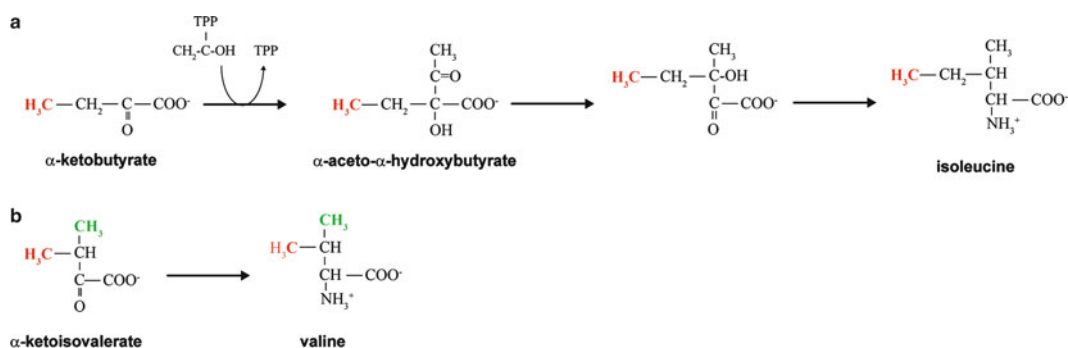


Fig. 4.5 Synthesis of the amino acids (a) Ile and (b) Val from the precursors α -ketobutyrate and α -ketoisovalerate, respectively. The methyl group of α -ketobutyrate is highlighted in red and the two methyl groups of α -ketoisovalerate are shown in red and green. Both or either can be labeled with ^{13}C . The methyl groups of Leu will be labeled in the same manner as the ones in Val if α -ketoisovalerate is added to the growth medium

specifically labeled with ^{13}C at the methyl groups to the growth medium [54]. This is usually referred to as ILV labeling and is shown in Fig. 4.5. The methyl groups of Ile δ 1, Leu and Val are labeled to 90% if the precursors are supplied in concentrations of 50 mg/L for α -ketobutyrate and 100 mg/L for α -ketoisovalerate 1 h prior to induction of protein expression. Although these compounds can potentially be degraded into precursors for other amino acids the authors noticed essentially no labeling at other positions. A very useful feature of the method is that the labeling of the methyl groups can be customized. In addition of having all methyl groups $^{13}\text{CH}_3$ it is also possible to have them $^{13}\text{CH}_2\text{D}$ or $^{13}\text{CHD}_2$. One can also label different methyl groups differently. By using α -ketoisovalerate labeled with $^{13}\text{CH}_3$ at one methyl group and with $^{12}\text{CD}_3$ at the other, so that only the *proR* or *proS* methyl groups of Leu and Val are detectable, resulting in less crowded spectra. Finally, for applications involving high molecular weight proteins non-methyl positions of α -ketoisovalerate can be deuterated in-house by incubation at elevated pH [54]. Using this approach it is possible to record relaxation experiments for systems as large as the proteasome 20S core particle of 670 kDa [55].

Recently Ruschak et al. suggested a method to instead label Ile γ 2 to enable measurements at that position in large proteins [56]. The scheme is based on the precursor α -aceto- α -hydroxybutyrate that is $^{13}\text{C}/^1\text{H}$ labeled only at the relevant methyl group and $^{12}\text{C}/^2\text{H}$ labeled elsewhere. For reasons of stability the compound is purchased in its ethyl ester form and de-esterified by incubation with esterase. An amount corresponding to 100 mg/L of the acid form is added to the growth medium. Contrary to what is observed for the ILV labeling scheme, scrambling leads to the presence of weak correlations of *proR* Val γ and Leu δ [56]. However, these do not complicate the interpretation of the spectra considerably.

Certain relaxation experiments involving methyl side-chains are feasible for uniformly ^{13}C or $^{13}\text{C}/^{15}\text{N}$ labeled samples. Brath et al. produced a uniformly $^{13}\text{C}/^{15}\text{N}$ -labeled, partially ^2H labeled sample of FKBP12 by over expression in M9 medium supplemented with 50% D_2O . They used this sample to measure $R_{1\rho}$ in methyl groups of the $^{13}\text{CHD}_2$ variety [57]. In this case evolution of the strong three-bond $^{13}\text{C}^{\text{methyl}}\text{-}^{13}\text{C}\alpha$ couplings in Leu residues is a concern for certain combinations of offsets and spin-lock field strengths. It should be added that other ratios of $\text{H}_2\text{O}/\text{D}_2\text{O}$ ratios during over expression, for instance 100% D_2O , also lead to a large fraction of $^{13}\text{CHD}_2$ isotopomers.

4.5.2.5 Carbon Positions in Aromatic Side-Chains

Besides methyl groups the other most common residues in the protein interior are the side-chains of the aromatic residues. Additionally the side-chain of His is for instance frequently located at the active site of enzymes and is involved in catalysis. Despite their important role for protein structure

and function, NMR relaxation experiments involving aromatic side-chains are rare and only a few applications and one selective labeling scheme will be reported here.

Hass et al. have exploited the fact that the C ϵ 1 position of His residues is isolated from scalar couplings to other carbon positions and thus used a uniformly $^{13}\text{C}/^{15}\text{N}$ labeled sample to measure CPMG dispersions on the protein plastocyanin. The extracted chemical shift differences agreed well with those obtained from chemical shift titrations [58].

[1- ^{13}C]-glucose was used to label aromatic side-chains of Phe and Tyr at C δ , His at C δ 2 and C ϵ 1 and Trp C δ 1 and C ϵ 3 (and C ϵ 2 although it cannot be seen in HSQC type experiments). The labeling efficiency is about 50%. This labeling scheme allowed relaxation dispersions to be measured for the aromatic side-chains of the E140Q mutant of the C-terminal domain of calmodulin [59]. Boyer and Lee used this labeling scheme to also probe fast dynamics at 13 aromatic positions for the protein eglin C to compare differences in dynamics between the wild type protein and the V54A mutant [60].

4.5.3 Proton Positions

The main benefit of measuring relaxation dispersions for protons is that their high magnetogyric ratio facilitates high repetition rates and high effective fields in CPMG and $R_{1\rho}$ experiments, respectively. Motions that are one order of magnitude faster than can be measured in ^{15}N relaxation dispersion experiments may thus be captured. The main complications when measuring relaxation rates for protons are their sizable dipolar and scalar couplings with remote protons. Both these difficulties can be reduced significantly by perdeuteration or partial deuteration and by including refocusing elements for homonuclear couplings in the pulse sequences. Labeling schemes and applications for relaxation experiments involving ^1HN , $^1\text{H}\alpha$ and $^1\text{H}^{\text{methyl}}$ will now follow.

4.5.3.1 Amide Proton Positions

The amide proton is coupled to the alpha proton with a coupling constant that ranges from 3 to 12 Hz depending on secondary structure [61]. Since prohibitively long pulses are needed to refocus this coupling during a CPMG pulse train used to measure transverse relaxation rates, it is necessary to remove it by perdeuteration [62, 63]. The labeling scheme for these experiments is thus M9 medium supplemented with 1 g/L $^{15}\text{NH}_4\text{Cl}$ and 3 g/L [$^{13}\text{C}_6, ^2\text{H}_7$]-glucose in 100% D_2O . It has been shown that accurate protein excited state chemical shifts can be extracted from CPMG experiments performed on such samples [41]. An excellent alternative to CPMG experiments for the amide proton that can be used for both protonated and perdeuterated samples is rotating-frame relaxation experiments [64–66].

4.5.3.2 Alpha Proton Positions

For the alpha protons similar problems as for the amide protons exist. However, when running CPMG dispersion experiments one must also consider couplings to beta protons. Because of the small separation in chemical shifts between $^1\text{H}\alpha$ and $^1\text{H}\beta$ it is not possible to use pulses that are selective to $^1\text{H}\alpha$ in the CPMG pulse train. This means that if the beta positions are protonated artifacts similar to the ones that were present in the carbonyl CPMG experiment result. However in this case the problem exists for all residue types and is worse because the magnetization can be further transferred to the gamma position. Even if a refocusing element, akin to the one used in the ^{13}CO dispersion experiment, is included, artifact-free CPMG dispersions are not possible for fully protonated samples. The solution was to combine this strategy with a selective labeling scheme where the protein was produced by

over expression in a medium containing 3 g/L [$^{13}\text{C}_6$, $^2\text{H}_7$]-glucose as the carbon source and 50% D_2O /50% H_2O as solvent [67]. This leads to deuteration at beta positions of 50–88% depending on residue type. Unfortunately, it also leads to an overall sensitivity loss of 50% since protonation at alpha positions is decreased by 50% for all residue types. Using this labeling scheme in combination with a refocusing element in the middle of the relaxation delay, it was possible to extract accurate chemical shifts of protein excited states [67].

4.5.3.3 Methyl Proton Positions

Mulder and coworkers have developed a CPMG relaxation dispersion experiment that measures millisecond dynamics on $^{13}\text{CHD}_2$ groups [68]. They achieve the labeling by expressing calbindin $\text{D}_{9\text{k}}$ in a medium supplemented with protonated 2 g/L [$^{13}\text{C}_6$]-glucose in D_2O as described [69]. The experiment was also applied to the transcriptional activator NtrC^r . In this case [$1\text{-}^{13}\text{C}$]-glucose was the carbon source. The benefit of this is that non-constant time evolution NMR experiments can be employed, which may increase overall sensitivity for large proteins despite the fact that the methyl groups are only labeled to 50%. Kay and coworkers instead used an ILV labeled sample to measure these dynamics on the 20S proteasome core particle [70]. It should be noted that $^{13}\text{CHD}_2$ groups, especially in a highly deuterated background and with other carbon positions being ^{12}C , are sensitive probes for measurements of fast dynamics because of very favorable relaxation properties and because that no cross-correlation effects complicate relaxation behavior.

4.5.4 Deuterium Positions

Since deuterium is a spin $I=1$ nucleus, its dominating relaxation mechanism is the quadrupolar interaction. This mechanism dominates to the extent that other relaxation mechanisms, including chemical exchange, can be safely neglected, which simplifies the analysis. Furthermore, in this case auto-relaxation rates can be measured for five different operators leading to high levels of confidence in the extracted parameters. Because of the large intrinsic relaxation rates, relaxation measurements involving deuterium spins are in practice limited to methyl groups. Kay and coworkers used a uniformly ^{13}C labeled, fractionally deuterated sample and pulse sequences that select for the CH_2D isotopomer to measure the five relaxation rates in order to calculate order parameters for side-chains of the B1 domain of peptostreptococcal protein L [71, 72]. Wand and coworkers have used the same approach to characterize side-chain dynamics in calmodulin [73]. Of course, other labeling schemes, like ILV labeling with $^{13}\text{CH}_2\text{D}$ labeled methyl groups, can also be employed for measurements of these relaxation rates. This has been used to probe dynamics of the 20S core particle of the proteasome [55].

4.6 Labeling by Cell-Free Synthesis

Rather than expressing the protein in a cell, the proteins for NMR applications can also be expressed *in vitro* [74]. The DNA or mRNA for the target protein is added to a cell extract containing the transcription and translation machinery of the cell, along with a variety of other compounds including amino acids, nucleoside triphosphates (NTPs) and several enzymes. A way to regenerate energy is also required. The reaction mixture is typically only a few μL -mL large, and yields of several mg of protein per mL of reaction mixture can be achieved. Chaperones, detergents and other compounds that facilitate folding can also be added.

Cell-free protein expression has several advantages both for creating specific isotopic labeling schemes, but also for efficient expression, generally. One is speed since the entire over expression protocol is normally conducted in a few hours, compared to one to several days when using over expression in *E. coli*. Additionally the purification protocol is usually simpler. Another important aspect is that because of the short time of expression and more well-defined conditions, there is less scrambling so that more of the label ends up at the desired place. It is very easy to label individual amino acids simply by adding them to the reaction mixture in labeled form and adding the other amino acids unlabeled. Scrambling due to *E. coli* metabolism is minimized and can often be further reduced by adding specific inhibitors to the reaction mixture. Although labeled amino acids may be quite expensive, the small amounts required for cell-free protein expression makes this method competitive also from a financial point of view. If only one or a few of the amino acids are supplied in labeled form, costs are reduced further. Cell-free protein expression can be very useful for proteins which do not express well in cells, for example because of toxicity. Cell-free expression is also proving to be successful for membrane proteins which can be very difficult to express in large amounts in cells [75].

A powerful application of cell-free synthesis is stereo-array isotope labeling (SAIL) [76]. This protocol produces alternate labeling in the following way. First, stereo-selective replacement of one ^1H in methylene groups by ^2H ; second, replacement of two ^1H in each methyl group by ^2H ; third, stereo-selective modification of the prochiral methyl groups of Leu and Val such that one methyl is $^{12}\text{CD}_3$ and the other is $^{13}\text{CHD}_2$; and last, labeling of six-membered aromatic rings by alternating ^{12}CD and ^{13}CH moieties. Although the method was developed for structure determination, it is easy to imagine applications involving relaxation as well. For instance, the labeling scheme should be optimal for probing dynamics at aromatic side-chains. Unfortunately the method is still too expensive to be an option for most laboratories.

4.7 Concluding Remarks

As should be evident from this chapter, relaxation experiments are feasible for many different nuclear species and positions in proteins. For many positions, uniform labeling with ^{15}N , $^{15}\text{N}/^{13}\text{C}$ or $^{15}\text{N}/^{13}\text{C}/^2\text{H}$ is adequate for obtaining robust results. These include ^{15}N and ^{13}CO at backbone and side-chain positions as well as ^1HN at the protein backbone. In other cases, it is necessary to use selective strategies to remove scalar and dipolar interactions. The selective labeling protocols range from being very simple, like substituting selectively labeled glucose for unlabeled or uniformly labeled glucose, to being more intricate, like using selectively labeled glycerol as the carbon source in genetically engineered bacterial strains or supplementing the growth medium with customized precursors for a subset of the amino acids.

The original methods of measuring R_1 , R_2 and NOE in uniformly ^{15}N labeled samples have been, and still are, extremely useful for determining the diffusion tensor and characterizing sub-nanosecond motions of proteins and CPMG experiments recorded for these protein samples have been instrumental in increasing our understanding of processes like protein folding, ligand binding and enzymatic catalysis. It is however increasingly clear that relaxation experiments probing dynamics at other sites provide complementary information and in some cases has opened an avenue to understanding processes and characterizing intermediate protein states that have previously eluded us. For instance, by using excited state chemical shifts extracted from CPMG experiments for ^{15}N , ^1HN , $^1\text{H}\alpha$, $^{13}\text{C}\alpha$ and ^{13}CO as the restraints in structure calculations it is now possible to determine structures of transiently populated folding intermediates [77] and by using ILV labeled samples it is possible to characterize dynamics of high molecular weight systems and to correlate these dynamics with function [55]. Although the development of labeling schemes of the last decade has enabled all this it will be exciting to continue to improve these methods to be able to tackle new biological questions during the next decade.

References

1. Lipari G, Szabo A (1982) Model-free approach to the interpretation of nuclear magnetic-resonance relaxation in macromolecules. 1. Theory and range of validity. *J Am Chem Soc* 104:4546–4559
2. Lipari G, Szabo A (1982) Model-free approach to the interpretation of nuclear magnetic-resonance relaxation in macromolecules. 2. Analysis of experimental results. *J Am Chem Soc* 104:4559–4570
3. Clore GM, Szabo A, Bax A, Kay LE, Driscoll PC, Gronenborn AM (1990) Deviations from the simple two-parameter model-free approach to the interpretation of ^{15}N nuclear magnetic relaxation of proteins. *J Am Chem Soc* 112:4989–4991
4. Loria JP, Rance M, Palmer AG 3rd (1999) A relaxation-compensated Carr-Purcell-Meiboom-Gill sequence for characterizing chemical exchange by NMR spectroscopy. *J Am Chem Soc* 121:2331–2332
5. Hansen DF, Vallurupalli P, Kay LE (2008) An improved ^{15}N relaxation dispersion experiment for the measurement of millisecond time-scale dynamics in proteins. *J Phys Chem B* 112:5898–5904
6. Akke M, Palmer AG 3rd (1996) Monitoring macromolecular motions on microsecond to millisecond time scales by $R_{1\rho}$ - R_1 constant relaxation time NMR spectroscopy. *J Am Chem Soc* 118:911–912
7. Korzhnev DM, Orekhov VY, Dahlquist FW, Kay LE (2003) Off-resonance $R_{1\rho}$ relaxation outside of the fast exchange limit: an experimental study of a cavity mutant of T4 lysozyme. *J Biomol NMR* 26:39–48
8. Bloch F (1946) Nuclear induction. *Phys Rev* 70:460–474
9. Abragam A (1961) Principles of nuclear magnetism. Oxford University Press, Oxford
10. Redfield AG (1957) On the theory of relaxation processes. *IBM J Res Dev* 1:19–31
11. Kay LE, Torchia DA, Bax A (1989) Backbone dynamics of proteins as studied by ^{15}N inverse detected heteronuclear NMR-spectroscopy – application to staphylococcal nuclease. *Biochemistry* 28:8972–8979
12. Farrow NA, Muhandiram R, Singer AU, Pascal SM, Kay CM, Gish G, Shoelson SE, Pawson T, Formankay JD, Kay LE (1994) Backbone dynamics of a free and a phosphopeptide-complexed Src homology-2 domain studied by ^{15}N NMR relaxation. *Biochemistry* 33:5984–6003
13. Boehr DD, McElheny D, Dyson HJ, Wright PE (2006) The dynamic energy landscape of dihydrofolate reductase catalysis. *Science* 313:1638–1642
14. Sugase K, Dyson HJ, Wright PE (2007) Mechanism of coupled folding and binding of an intrinsically disordered protein. *Nature* 447:1021–1025
15. Korzhnev DM, Salvatella X, Vendruscolo M, Di Nardo AA, Davidson AR, Dobson CM, Kay LE (2004) Low-populated folding intermediates of Fyn SH3 characterized by relaxation dispersion NMR. *Nature* 430:586–590
16. Carr HY, Purcell EM (1954) Effects of diffusion on free precession in nuclear magnetic resonance experiments. *Phys Rev* 94:630–638
17. Meiboom S, Gill D (1958) Modified spin-echo method for measuring nuclear relaxation times. *Rev Sci Instrum* 29:688–691
18. Jones GP (1966) Spin-lattice relaxation in the rotating frame: weak collision case. *Phys Rev* 148:332–335
19. Davis DG, Perlman ME, London RE (1994) Direct measurements of the dissociation-rate constant for inhibitor-enzyme complexes via the $T_{1\rho}$ and T_2 (CPMG) methods. *J Magn Reson Ser B* 104:266–275
20. McConnell HM (1958) Reaction rates by nuclear magnetic resonance. *J Chem Phys* 28:430–431
21. Palmer AG 3rd, Kroenke CD, Loria JP (2001) Nuclear magnetic resonance methods for quantifying microsecond-to-millisecond motions in biological macromolecules. *Methods Enzymol* 339:204–238
22. Palmer AG 3rd, Massi F (2006) Characterization of the dynamics of biomacromolecules using rotating-frame spin relaxation NMR spectroscopy. *Chem Rev* 106:1700–1719
23. Jeener J, Meier MH, Bachmann P, Ernst RR (1979) Investigation of exchange processes by 2-dimensional NMR spectroscopy. *J Chem Phys* 71:4546–4553
24. Cornilescu G, Delaglio F, Bax A (1999) Protein backbone angle restraints from searching a database for chemical shift and sequence homology. *J Biomol NMR* 13:289–302
25. Shen Y, Lange O, Delaglio F, Rossi P, Aramini JM, Liu GH, Eletsky A, Wu YB, Singarapu KK, Lemak A, Ignatchenko A, Arrowsmith CH, Szyperski T, Montelione GT, Baker D, Bax A (2008) Consistent blind protein structure generation from NMR chemical shift data. *Proc Natl Acad Sci USA* 105:4685–4690
26. Cavalli A, Salvatella X, Dobson CM, Vendruscolo M (2007) Protein structure determination from NMR chemical shifts. *Proc Natl Acad Sci USA* 104:9615–9620
27. Korzhnev DM, Neudecker P, Mittermaier A, Orekhov VY, Kay LE (2005) Multiple-site exchange in proteins studied with a suite of six NMR relaxation dispersion experiments: an application to the folding of a Fyn SH3 domain mutant. *J Am Chem Soc* 127:15602–15611
28. Skrynnikov NR, Konrat R, Muhandiram DR, Kay LE (2000) Relative orientation of peptide planes in proteins is reflected in carbonyl-carbonyl chemical shift anisotropy cross-correlated spin relaxation. *J Am Chem Soc* 122:7059–7071

29. Kloiber K, Konrat R (2000) Measurement of the protein backbone dihedral angle phi based on quantification of remote CSA/DD interference in inter-residue $^{13}\text{C}'(\text{i} - 1)\text{-}^{13}\text{C}\alpha(\text{i})$ multiple-quantum coherences. *J Biomol NMR* 17:265–268
30. Kloiber K, Konrat R (2000) Differential multiple-quantum relaxation arising from cross-correlated time-modulation of isotropic chemical shifts. *J Biomol NMR* 18:33–42
31. Voet D, Voet JG (1995) *Biochemistry*. Wiley, Hoboken
32. Gottschalk G (1986) *Bacterial metabolism*. Springer, New York
33. Maniatis T, Sambrook J, Fritsch EF (1982) *Molecular cloning: a laboratory manual*. Cold Spring Harbor Laboratory, Cold Spring Harbor, pp 68–69
34. Lundström P, Vallurupalli P, Hansen DF, Kay LE (2009) Isotope labeling methods for studies of excited protein states by relaxation dispersion NMR spectroscopy. *Nat Protoc* 4:1641–1648
35. Middelberg APJ (2002) Preparative protein refolding. *Trends Biotechnol* 20:437–443
36. Mulder FAA, Skrynnikov NR, Hon B, Dahlquist FW, Kay LE (2001) Measurement of slow (μs -ms) time scale dynamics in protein side chains by ^{15}N relaxation dispersion NMR spectroscopy: application to Asn and Gln residues in a cavity mutant of T4 lysozyme. *J Am Chem Soc* 123:967–975
37. Korzhnev DM, Skrynnikov NR, Millet O, Torchia DA, Kay LE (2002) An NMR experiment for the accurate measurement of heteronuclear spin-lock relaxation rates. *J Am Chem Soc* 124:10743–10753
38. Ishima R, Baber J, Louis JM, Torchia DA (2004) Carbonyl carbon transverse relaxation dispersion measurements and ms- μs timescale motion in a protein hydrogen bond network. *J Biomol NMR* 29:187–198
39. Lundström P, Hansen DF, Kay LE (2008) Measurement of carbonyl chemical shifts of excited protein states by relaxation dispersion NMR spectroscopy: comparison between uniformly and selectively (^{13}C) labeled samples. *J Biomol NMR* 42:35–47
40. Mulder FAA, Akke M (2003) Carbonyl ^{13}C transverse relaxation measurements to sample protein backbone dynamics. *Magn Reson Chem* 41:853–865
41. Hansen DF, Vallurupalli P, Lundström P, Neudecker P, Kay LE (2008) Probing chemical shifts of invisible states of proteins with relaxation dispersion NMR spectroscopy: how well can we do? *J Am Chem Soc* 130:2667–2675
42. Hansen AL, Kay LE (2011) Quantifying millisecond time-scale exchange in proteins by CPMG relaxation dispersion NMR spectroscopy of side-chain carbonyl groups. *J Biomol NMR* 50:347–355
43. Wand AJ, Bieber RJ, Urbauer JL, McEvoy RP, Gan ZH (1995) Carbon relaxation in randomly fractionally ^{13}C -enriched proteins. *J Magn Reson Ser B* 108:173–175
44. LeMaster DM, Kushlan DM (1996) Dynamical mapping of E. coli thioredoxin via ^{13}C NMR relaxation analysis. *J Am Chem Soc* 118:9255–9264
45. Castellani F, van Rossum B, Diehl A, Schubert M, Rehbein K, Oschkinat H (2002) Structure of a protein determined by solid-state magic-angle-spinning NMR spectroscopy. *Nature* 420:98–102
46. Lundström P, Teilum K, Carstensen T, Bezsonova I, Wiesner S, Hansen DF, Religa TL, Akke M, Kay LE (2007) Fractional ^{13}C enrichment of isolated carbons using [$1\text{-}^{13}\text{C}$] or [$2\text{-}^{13}\text{C}$] glucose facilitates the accurate measurement of dynamics at backbone C^α and side-chain methyl positions in proteins. *J Biomol NMR* 38:199–212
47. Yamazaki T, Muhandiram R, Kay LE (1994) NMR experiments for the measurement of carbon relaxation properties in highly enriched, uniformly ^{13}C , ^{15}N -labeled proteins – application to $^{13}\text{C}^\alpha$ carbons. *J Am Chem Soc* 116:8266–8278
48. Lundström P, Akke M (2005) Microsecond protein dynamics measured by $^{13}\text{C}^\alpha$ rotating-frame spin relaxation. *Chembiochem* 6:1685–1692
49. Lundström P, Lin H, Kay LE (2009) Measuring $^{13}\text{C}^\beta$ chemical shifts of invisible excited states in proteins by relaxation dispersion NMR spectroscopy. *J Biomol NMR* 44:139–155
50. Skrynnikov NR, Mulder FAA, Hon B, Dahlquist FW, Kay LE (2001) Probing slow time scale dynamics at methyl-containing side chains in proteins by relaxation dispersion NMR measurements: application to methionine residues in a cavity mutant of T4 lysozyme. *J Am Chem Soc* 123:4556–4566
51. Korzhnev DM, Religa TL, Lundström P, Fersht AR, Kay LE (2007) The folding pathway of an FF domain: characterization of an on-pathway intermediate state under folding conditions by ^{15}N , $^{13}\text{C}^\alpha$ and ^{13}C -methyl relaxation dispersion and $^1\text{H}/^2\text{H}$ -exchange NMR spectroscopy. *J Mol Biol* 372:497–512
52. Lundström P, Vallurupalli P, Religa TL, Dahlquist FW, Kay LE (2007) A single-quantum methyl ^{13}C -relaxation dispersion experiment with improved sensitivity. *J Biomol NMR* 38:79–88
53. Mulder FAA, Hon B, Mittermaier A, Dahlquist FW, Kay LE (2002) Slow internal dynamics in proteins: application of NMR relaxation dispersion spectroscopy to methyl groups in a cavity mutant of T4 lysozyme. *J Am Chem Soc* 124:1443–1451
54. Goto NK, Gardner KH, Mueller GA, Willis RC, Kay LE (1999) A robust and cost-effective method for the production of Val, Leu, Ile ($\delta 1$) methyl-protonated ^{15}N -, ^{13}C -, ^2H -labeled proteins. *J Biomol NMR* 13:369–374
55. Sprangers R, Kay LE (2007) Quantitative dynamics and binding studies of the 20S proteasome by NMR. *Nature* 445:618–622

56. Ruschak AM, Velyvis A, Kay LE (2010) A simple strategy for ^{13}C , ^1H labeling at the Ile-gamma 2 methyl position in highly deuterated proteins. *J Biomol NMR* 48:129–135
57. Brath U, Akke M, Yang DW, Kay LE, Mulder FAA (2006) Functional dynamics of human FKBP12 revealed by methyl ^{13}C rotating frame relaxation dispersion NMR spectroscopy. *J Am Chem Soc* 128:5718–5727
58. Hass MA, Hansen DF, Christensen HE, Led JJ, Kay LE (2008) Characterization of conformational exchange of a histidine side chain: protonation, rotamerization, and tautomerization of His61 in plastocyanin from *Anabaena variabilis*. *J Am Chem Soc* 130:8460–8470
59. Teilmann K, Brath U, Lundström P, Akke M (2006) Biosynthetic ^{13}C labeling of aromatic side chains in proteins for NMR relaxation measurements. *J Am Chem Soc* 128:2506–2507
60. Boyer JA, Lee AL (2008) Monitoring aromatic picosecond to nanosecond dynamics in proteins via (^{13}C) relaxation: expanding perturbation mapping of the rigidifying core mutation, V54A, in Eglin C. *Biochemistry* 47:4876–4886
61. Schmidt JM, Blumel M, Löhr F, Rüterjans H (1999) Self-consistent (^3J) coupling analysis for the joint calibration of Karplus coefficients and evaluation of torsion angles. *J Biomol NMR* 14:1–12
62. Ishima R, Torchia DA (2003) Extending the range of amide proton relaxation dispersion experiments in proteins using a constant-time relaxation-compensated CPMG approach. *J Biomol NMR* 25:243–248
63. Orekhov VY, Korzhnev DM, Kay LE (2004) Double- and zero-quantum NMR relaxation dispersion experiments sampling millisecond time scale dynamics in proteins. *J Am Chem Soc* 126:1886–1891
64. Ishima R, Wingfield PT, Stahl SJ, Kaufman JD, Torchia DA (1998) Using amide ^1H and ^{15}N transverse relaxation to detect millisecond time-scale motions in perdeuterated proteins: application to HIV-1 protease. *J Am Chem Soc* 120:10534–10542
65. Lundström P, Akke M (2005) Off-resonance rotating-frame amide proton spin relaxation experiments measuring microsecond chemical exchange in proteins. *J Biomol NMR* 32:163–173
66. Eichmüller C, Skrynnikov NR (2005) A new amide proton $R_{1\rho}$ experiment permits accurate characterization of microsecond time-scale conformational exchange. *J Biomol NMR* 32:281–293
67. Lundström P, Hansen DF, Vallurupalli P, Kay LE (2009) Accurate measurement of alpha proton chemical shifts of excited protein states by relaxation dispersion NMR spectroscopy. *J Am Chem Soc* 131:1915–1926
68. Otten R, Villali J, Kern D, Mulder FAA (2010) Probing microsecond time scale dynamics in proteins by methyl ^1H Carr-Purcell-Meiboom-Gill relaxation dispersion NMR measurements. Application to activation of the signaling protein NtrC(r). *J Am Chem Soc* 132:17004–17014
69. LeMaster DM (1990) Deuterium labeling in NMR structural analysis of larger proteins. *Q Rev Biophys* 23:133–174
70. Baldwin AJ, Religa TL, Hansen DF, Bouvignies G, Kay LE (2010) $^{13}\text{CHD}_2$ methyl group probes of millisecond time scale exchange in proteins by ^1H relaxation dispersion: an application to proteasome gating residue dynamics. *J Am Chem Soc* 132:10992–10995
71. Millet O, Muhandiram DR, Skrynnikov NR, Kay LE (2002) Deuterium spin probes of side-chain dynamics in proteins. 1. Measurement of five relaxation rates per deuteron in ^{13}C -labeled and fractionally ^2H -enriched proteins in solution. *J Am Chem Soc* 124:6439–6448
72. Skrynnikov NR, Millet O, Kay LE (2002) Deuterium spin probes of side-chain dynamics in proteins. 2. Spectral density mapping and identification of nanosecond time-scale side-chain motions. *J Am Chem Soc* 124:6449–6460
73. Frederick KK, Marlow MS, Valentine KG, Wand AJ (2007) Conformational entropy in molecular recognition by proteins. *Nature* 448:325–329
74. Kigawa T, Muto Y, Yokoyama S (1995) Cell-free synthesis and amino acid-selective stable isotope labeling of proteins for NMR analysis. *J Biomol NMR* 6:129–134
75. Schwarz D, Daley D, Beckhaus T, Dotsch V, Bernhard F (2010) Cell-free expression profiling of *E. coli* inner membrane proteins. *Proteomics* 10:1762–1779
76. Kainosho M, Torizawa T, Iwashita Y, Terauchi T, Ono AM, Guntert P (2006) Optimal isotope labelling for NMR protein structure determinations. *Nature* 440:52–57
77. Korzhnev DM, Religa TL, Banachewicz W, Fersht AR, Kay LE (2010) A transient and low-populated protein-folding intermediate at atomic resolution. *Science* 329:1312–1316